Vibrational structures of predissociating methylamines (CH_3NH_2 and CH_3ND_2) in $\tilde{A}$ states: Free internal rotation of CH_3 with respect to NH_2

Sun Jong Baek, Kyo-Won Choi, Young S. Choi, and Sang Kyu Kim[a)]
Department of Chemistry, Inha University, Incheon 402-751, Republic of Korea

(Received 20 June 2002; accepted 10 September 2002)

Resonantly-enhanced one-color two-photon (1+1) ionization spectra of jet-cooled methylamines (CH_3NH_2 and CH_3ND_2) reveal the vibrational structures of these molecules in predissociative $\tilde{A}$ states. Rotational fine structure is clearly resolved for CH_3ND_2 at the origin and first wagging vibrational level in the excited state. The spectral linewidth becomes homogeneously broadened to give only vibrationally resolved spectral features for the higher vibrational energy levels of CH_3ND_2 ($\tilde{A}$). From the spectral analysis of the $\tilde{A}-X$ transition of CH_3ND_2, it is found that the methyl moiety rotates nearly freely about the C–N axis with respect to the amino group in the $\tilde{A}$ state, indicating that the removal of an electron from the nonbonding orbital of N is responsible for the free internal rotation. Vibrational levels are only barely resolved in the $\tilde{A}-X$ excitation spectrum of CH_3NH_2 due to severe homogeneous line-broadening, indicating ultrashort lifetimes of ~0.4 ps for predissociating CH_3NH_2 molecules in the $\tilde{A}$ state. Spectral interpretation of the $\tilde{A}-X$ excitation spectrum of CH_3NH_2 is carried out by the comparison with that of CH_3ND_2, giving the confirmative vibrational assignment of methylamines in $\tilde{A}$ states for the first time. The dramatic difference of CH_3NH_2 and CH_3ND_2 in their lifetimes in $\tilde{A}$ states suggests that the major dissociation channel of the excited methylamine may be the N–H (or D) bond dissociation. © *2002 American Institute of Physics.* [DOI: 10.1063/1.1518005]

I. INTRODUCTION

Primary amines are ubiquitous in organic and biological compounds, and they are frequently used as common Lewis bases in many organic syntheses. The simplest primary amine is methylamine. Because of its simplicity and importance in chemistry and biology, methylamine has been used as a model compound to study the effect of electronic configuration on molecular structures and/or reaction dynamics occurring on various excited states.[1,2] However, unlike ammonia, of which spectroscopy and dynamics were thoroughly studied,[3–6] the methylamine structure and dynamics in the excited state have not been intensively investigated yet, even though some interesting dissociation dynamics features occurring on the excited methylamine were revealed through recent nice studies by numerous research groups.[7–10] One of the main obstacles in the further detailed study of the methylamine dynamics in this direction has been the relatively poor quantum-mechanical characterization of the reactant molecule, methylamine in the $\tilde{A}$ state.[1,2]

The first UV absorption band of methylamine (190–240 nm) is ascribed to the excitation of an electron in the lone-pair of the N atom to the 3*s* Rydberg state. The excited Rydberg state couples to other electronic states correlating to different products. Energetically accessible reaction channels include the reaction pathways giving CH_3NH+H, CH_2NH_2+H, CH_3+NH_2, and CH_2NH+H_2 products.[8–10] These four reactions occur competitively, and their relative yields depend not only on dissociation energetics but also on detailed shapes of potential energy surfaces along the reaction pathways. Therefore, it would be very interesting to investigate the effect of the quantum-mechanical state of the reactant on the final products in terms of their relative yields and product state distributions. Spectroscopy of methylamine in the ground electronic state has been thoroughly investigated using far-infrared and microwave absorption spectroscopy, to give accurate rotational constants, vibrational frequencies, and rovibrational coupling terms.[11,12] For the first electronically excited state of methylamines, however, even the position of spectral origin seems to still be controversial.[1,2,13–16] In 1937, Förster and Jurgens reported 41 680 cm^{-1} as the spectral origin of CH_3NH_2.[13] Later, Tsuboi *et al.* reported that the CH_3NH_2 absorption spectrum consists of the origin at 41 715 cm^{-1} and progression and combination bands due to NH_2 wag at ~650 cm^{-1} and CH_3 rock at ~1000 cm^{-1}.[15,16] Those studies, however, were carried out at room temperature and spectra were taken with no mass resolution. More reliable spectra for the $\tilde{A}-X$ transition of methylamines were recently reported by Taylor and Bernstein in 1995.[2] They used (1+1) or (2+2) resonantly enhanced multiphoton ionization (REMPI) spectroscopy with efficient cooling to provide the relatively highly resolved excitation spectra of the CH_3NH_2 and its isotopic analogs. According to Taylor and Bernstein, spectral origins of methylamines are not observed due to severe structural change occurring upon the $\tilde{A}-X$ transition and optically active modes are NH_2 wag and scissor with associated vibrational frequencies of 642 and 1476 cm^{-1}, respectively.[2]

a)Author to whom correspondence should be addressed. Electronic mail: skkim@inha.ac.kr

However, REMPI spectra reported in Ref. 2 are mostly taken by the (2+2) transition with tight focusing of the laser beam on the molecular beam. Therefore, additional spectral features due to unknown multiphoton effect might possibly mislead the spectral interpretation.

In this work, we have used (1+1) one-color two-photon excitation scheme to obtain the REMPI spectra of CH_3NH_2 and CH_3ND_2 for the $\tilde{A}-X$ transition. We have obtained high-quality excitation spectra of these molecules at a very low temperature of ~3 K. We have found that the REMPI spectrum of CH_3ND_2 is rotationally resolved in the first two vibrational bands. More surprisingly, the CH_3 group is found to freely rotate with respect to the ND_2 moiety in the excited state of CH_3ND_2. A full analysis of the CH_3ND_2 excitation spectrum turns out to be extremely useful not only in establishing the long-time controversial vibrational assignment of the broad bands in the CH_3NH_2 spectrum but also in investigating underlying dynamics.

II. EXPERIMENT

A gaseous sample of methylamine (CH_3NH_2) was purchased from Aldrich and used without further purification. For the preparation of deuterated methylamine (CH_3ND_2), CH_3NH_2 was dissolved in D_2O and dehydrated in KOH solution. This exchange-dehydration process was carried out for several times for the preparation of the pure CH_3ND_2 sample. Samples were introduced to gas cylinders to prepare ~3% gas mixtures of methylamines in neon. The resultant gas mixture was expanded through a nozzle orifice (General Valve, 0.3 mm diameter) with a backing pressure of ~5 atm and a repetition rate of 10 Hz. The molecular beam was then skimmed through a 1-mm-diam skimmer in a differentially pumped vacuum chamber.

The third harmonic output of a Nd:YAG laser (Spectra-Physics, GCR-150) was used to pump a dye laser (Lambda-Physik, Scanmate 2) to generate the laser output in the 440–480 nm range, followed by the frequency doubling via a BBO crystal placed in a homemade autotracker to give the ultraviolet (UV) laser pulse, which was tunable in the 220–240 nm region. The laser wavelength was calibrated within ± 1 cm^{-1} using the optogalvanic signal from a hollow-cathode lamp (Ne). The UV laser pulse was overlapped with the molecular beam both in space and time to ionize methylamines by the (1+1) REMPI process. Molecular ions were repelled, accelerated, and drifted along the field-free region until they were detected by a multichannel-plate (MCP, Jordan) to give the REMPI signal. The signal was monitored as a function of the excitation UV wavelength to give REMPI spectra.

III. RESULTS AND DISCUSSION

The REMPI spectrum for the $\tilde{A}-X$ transition of CH_3NH_2 in the energy range of 41 500–44 500 cm^{-1} are shown in Fig. 1(a). The CH_3NH_2 excitation spectrum consists of a series of broad bands with unresolved structures in each band, similar to that reported in Ref. 2. Progression bands due to the NH_2 wagging mode and its combination bands with another vibrational mode are prominent. Since each band is quite poorly resolved, the overall or internal-rotational structure of the molecule could not be investigated. Dynamics behind the observed broad band of CH_3NH_2 ($\tilde{A}$) seem to be ambiguous, since the rotational temperature and constants cannot be deduced from the spectral analysis. On the contrary, the excitation spectrum of CH_3ND_2 in Fig. 1(b) is found to be dramatically different from that of CH_3NH_2 in terms of the linewidth of each band. In the first two vibrational bands, many sharp peaks are clearly resolved to give the rotational structure of CH_3ND_2 in $\tilde{A}$ state. This in turn indicates that broad bands observed in the CH_3NH_2 excitation spectrum are not due to insufficient cooling of the sample but actually due to homogeneous line-broadening of short-lived excited states. Therefore, we carry out the spectral analysis of the CH_3ND_2 spectrum first and then exploit molecular constants for the interpretation of the CH_3NH_2 excitation spectrum.

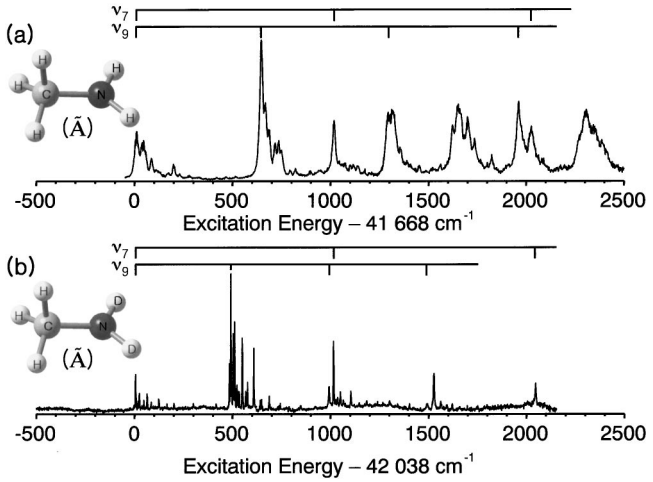

FIG. 1. (1+1) REMPI spectra of (a) CH_3NH_2 and (b) CH_3ND_2. The ν_7 and ν_9 modes represent CH_3 rocking and NH_2 (or ND_2) wagging modes, respectively. Bands located at ~1650 and ~2300 cm^{-1} in (a) are ascribed to $\nu_7+\nu_9$ and $\nu_7+2\nu_9$, respectively.

In the ground state, it is quite well known that the CH_3 group internally rotates with respect to the amino group with a torsional barrier of ~690 cm^{-1}.[11,12] This torsional barrier is expected to be decreased upon the $3s$-n excitation, since the nonbonding electron pair on N atom may play an important role in the hindered internal rotation. Experimental observation turns out to be much more dramatic. Rotationally resolved peaks in the 42 520–42 780 cm^{-1} region of the CH_3ND_2 excitation spectrum, Fig. 2(a), are almost perfectly reproduced by the free internal rotor model coupled with the overall rotation of the molecule, indicating that the CH_3–ND_2 internal rotation becomes nearly completely free in the $\tilde{A}$ state (*vide infra*). Of course, this experimental fact does not completely exclude the possibility of the existence of a very low hindered rotation barrier of a few cm^{-1}, and actually effects due to a low barrier seem to be reflected in Table I.

Methylamines in both X and $\tilde{A}$ states belong to nearly prolate symmetric top. Accordingly, the following energy relation deduced from a Hamiltonian based on the symmetric-top approximation is employed to predict energy levels asso-

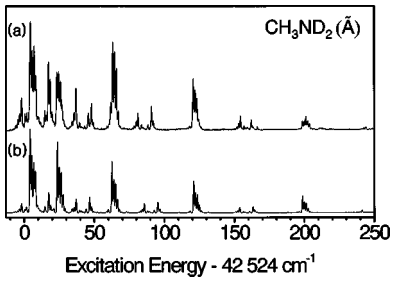

FIG. 2. (a) Experimentally observed excitation spectrum of CH_3ND_2 in the 42 500–42 800 cm^{-1} range compared with (b) the simulation (see the text for details).

ciated with various internal free-rotor states coupled with overall rotation,[17]

$$E(J,K_1,K_2)=BJ(J+1)-BK^2+A_1K_1^2+A_2K_2^2,$$
$$K=K_1+K_2, \tag{1}$$
$$A^{-1}=A_1^{-1}+A_2^{-1}.$$

Here, K is the overall rotational quantum number, while K_1 and K_2 are internal rotational quantum numbers for the CH_3 and ND_2 moieties, respectively. The axes of overall and internal rotations are assumed to be identical in the symmetric-top approximation. A and B are rotational constants of the molecule for the overall rotation of the molecule about the a and b (or c) principal axes, respectively. A_1 and A_2 are rotational constants of the CH_3 and ND_2 moieties for the internal rotation of two groups about the a axis, respectively.

In Fig. 2, many observed sharp peaks are compared with those obtained by the simulation. In the simulation, energy levels are calculated from Eq. (1), while relative transition intensities for different (J,K) values are calculated using the asymmetric rotor program.[18] Band intensities for various internal rotational quantum numbers are arbitrarily scaled just for the comparison with the experiment. A Gaussian function with an adjustable bandwidth (full width at half maximum $=\Delta E$) is convoluted for each transition to give the final simulated spectrum for the comparison with the experiment. As shown in Fig. 2, the simulation matches the experiment almost perfectly when $\Delta E=0.75$ cm^{-1}, $T_{rot}=3.6$ K, $B=0.66$, $A_1=4.86$, and $A_2=4.86$ cm^{-1}. Experimental and calculated peak positions only for some selected bands in Fig. 2 are listed with appropriate assignments in Table I. Slight mismatches should come from either the existence of a small torsional barrier or the failure of the symmetric-top approximation. The molecular constants used in the simulation are close to those ($B=0.677$, $A_1=5.175$, $A_2=5.617$ cm^{-1}) obtained by *ab initio* calculation (CIS) for the molecular structure of CH_3ND_2 in the $\tilde{A}$ state.[19] However, the smaller A_2 value obtained from the simulation compared to the *ab initio* value suggests the N–D bond length and/or D–N–D angle should be larger than theoretically predicted values.[19] The other point that should be mentioned is the bandwidth of 0.75 cm^{-1} used in the simulation, which is much larger than the experimental laser bandwidth of ~0.25 cm^{-1} in the UV region. According to a simple uncertainty relation of $\Delta E\cdot\Delta t\sim\hbar$, the lower limit for the lifetime of the CH_3ND_2 ($\tilde{A}$) at the first two vibrational bands is estimated to be ~6 ps. Rotationally resolved spectral features are observed only in the first two vibrational bands, Fig. 1. At the higher vibrational bands, the spectrum is no longer rotationally resolved due to severe line-broadening. This line-broadening should originate from the increase of the predissociation rate as the vibrational energy increases.

The identical energy expression, Eq. (1), is used for the simulation of the first band in the CH_3NH_2 spectrum. The simulation matches the experiment extremely well when $\Delta E=14$ cm^{-1}, $T_{rot}=3.6$ K, $B=0.785$, $A_t=4.86$, and $A_2=9.52$ cm^{-1}, as shown in Fig. 3. The A_2 value, which represents the internal rotational constant of NH_2, is close to twice that used for the CH_3ND_2 simulation, giving additional convincing evidence for the validity of the free internal-rotor model. The most dramatic change by the D/H isotopic sub-

TABLE I. Observed and calculated frequencies with assignments for bands in the 42 520–42 780 cm^{-1} region of the CH_3ND_2 excitation spectrum.

Obs freq[a] (cm^{-1})	Calc freq[b] (cm^{-1})	Excited states[c]				Ground states			Obs−calc (cm^{-1})
		J'	K'	K_1	K_2	J''	K_a''	K_c''	
−1.8	−1.9	1	0	0	0	1	1	1	0.1
	−1.8	2	0	0	0	2	1	2	0.0
4.4	4.2	1	1	0	1	1	0	1	0.2
	4.3	2	1	0	1	2	0	2	0.1
5.7	5.5	1	1	1	0	0	0	0	0.2
7.1	6.9	2	1	1	0	1	0	1	0.2
8.2	8.2	3	1	1	0	2	0	2	0.0
23.2	23.7	1	1	2	−1	1	0	1	−0.5
	23.7	2	1	2	−1	2	0	2	−0.5
24.5	25.0	1	1	2	−1	0	0	0	−0.5
25.8	26.3	2	1	2	−1	1	0	1	−0.5
36.9	37.0	1	0	−2	2	1	1	1	−0.1
	37.1	2	0	2	−2	2	1	2	−0.2
63.0	62.6	1	1	3	−2	1	0	1	0.4
	62.6	2	1	3	−2	2	0	2	0.4
64.4	63.9	1	1	3	−2	0	0	0	0.5
65.6	65.2	2	1	−2	3	1	0	1	0.4
81.1	85.6	1	0	−3	3	1	1	1	−4.5
	85.7	2	0	3	−3	2	1	2	−4.6
90.8	95.3	2	2	4	−2	1	1	0	−4.5
	95.3	2	2	−2	4	1	1	1	−4.5
120.6	120.9	1	1	4	−3	1	0	1	−0.3
	121.0	2	1	−3	4	2	0	2	−0.4
	121.0	3	1	4	−3	3	0	3	−0.4
121.9	122.2	1	1	4	−3	0	0	0	−0.3
123.2	123.6	2	1	4	−3	1	0	1	−0.4
154.3	153.7	1	0	−4	4	1	1	1	0.6
198.6	198.7	1	1	5	−4	1	0	1	−0.1
	198.7	2	1	−4	5	2	0	2	−0.1
200.0	200.0	1	1	−4	5	0	0	0	0.0
201.2	201.3	2	1	−4	5	1	0	1	−0.1

[a]For absolute transition frequencies, 42 524 cm^{-1} should be added. Peak positions are for maximum peak heights in the spectrum (Fig. 2). The correlation of observed and calculated frequencies here, therefore, is not exact. Rather, above observed peak positions are actually determined by the combination of several closely spaced transitions, which is clearly reflected in the simulation (see the text for details).

[b]See the text for parameters used for the simulation. For the ground state of CH_3ND_2, rotational constants of $A=2.607$, $B=0.6730$, and $C=0.6288$ cm^{-1} are used (Refs. 11 and 12).

[c]Since identical values for A_1 and A_2 are used in this particular calculation (see the text), only one pair of two possible pairs of (K_1,K_2) is shown.

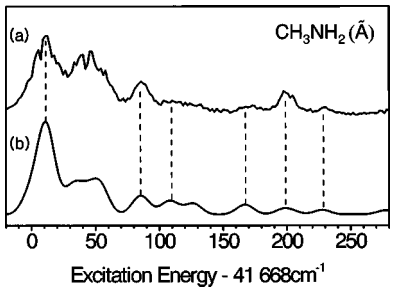

FIG. 3. (a) Experimentally observed excitation spectrum of CH_3NH_2 in the 41 650–41 950 cm^{-1} range compared with (b) the simulation (see the text for details).

stitution on the amino group is the large increase of the individual linewidth. The linewidth of 14 cm^{-1} corresponds to the lifetime of ~0.4 ps, indicating that the predissociation rate of CH_3NH_2 $(\tilde{A})$ is at least 10 times faster than that of CH_3ND_2 $(\tilde{A})$ at similar vibrational energies. This big difference in lifetimes of CH_3NH_2 and CH_3ND_2 strongly suggests that the major reaction channel of methylamine in the $\tilde{A}$ state is the N–H (or N–D) bond dissociation, which is expected to show the largest H/D isotope effect.

Now, for accurate vibrational assignments, one should assign the spectral origin correctly. As mentioned previously, the origin position has been quite controversial. The Bernstein group claimed that the origin is not observed due to a very low Franck–Condon factor of the origin transition, and the first observed band in the CH_3NH_2 spectrum corresponds to three quanta of NH_2 wagging mode.[2] However, the intensity of the first band is quite strong and the sudden drop of the Franck–Condon factor to absolute zero in the next lower quantum state is very unlikely. We have carefully measured excitation spectra in the wide energy region, and could not observe even tiny little bands at energies below the first observed bands in both spectra in Fig. 1. Therefore, in this work, the first bands in both CH_3NH_2 and CH_3ND_2 excitation spectra are ascribed to the origins for $\tilde{A}-X$ transitions. Precise band origins are determined in the simulations, Figs. 2 and 3, to give 41 669 and 42 038 cm^{-1} for the $\tilde{A}-X$ origins of CH_3NH_2 and CH_3ND_2, respectively. Vibrational assignments thereafter are quite straightforward. As indicated in Fig. 1, progression bands due to $NH_2(ND_2)$ wagging mode of CH_3NH_2 (CH_3ND_2) are clearly identified to give the corresponding fundamental vibrational frequencies of 636 (487) cm^{-1}. The band observed at 1008 (10) or 1011 (10) cm^{-1} above the origin of CH_3NH_2 or CH_3ND_2, respectively, is assigned to be the CH_3 rocking mode. Associated combination bands with NH_2 or ND_2 wag are also well identified in the CH_3NH_2 or CH_3ND_2 spectrum, respectively, in Fig. 1.

IV. CONCLUSION

In this work, the rotational-resolved excitation spectrum of deuterated methylamine, CH_3ND_2, is obtained for the first time to provide accurate molecular constants associated with overall and internal rotations. It is found that in the $\tilde{A}$ state, the methyl group rotates nearly freely with respect to the amino moiety, indicating that the removal of one of the electrons in the nonbonding orbital of N is responsible for the disappearance of the torsional barrier in the excited state. Broad features in the CH_3NH_2 spectrum, which had never been well understood before, are now perfectly interpreted using the free internal-rotor model. Lifetimes of excited states are deduced from linewidths of individual transitions to give ~6 and ~0.4 ps for zero-point levels of CH_3ND_2 and CH_3NH_2. Vibrational assignment of methylamine in the $\tilde{A}$ state is finally firmly established in this work, giving $\tilde{A}-X$ origins of 41 669 and 42 038 cm^{-1} for CH_3NH_2 and CH_3ND_2, respectively. The NH_2 wag at 636 and CH_3 rock at 1008(10) cm^{-1} are found to be optically active in the CH_3NH_2 spectrum. Similarly, ND_2 wag and CH_3 rock with their fundamental frequencies of 487 and 1011(10) cm^{-1}, respectively, are optically active in the CH_3ND_2 spectrum. Rovibrational structures of methylamines in the predissociative excited states, obtained in this work, would be extremely useful for the further study of reaction dynamics occurring from different quantum states of reactants.

ACKNOWLEDGMENTS

This work was financially supported by KOSEF (1999-1-121-001-5). S.J.B. and K.-W.C. thank the Brain-Korea 21 program for support. S.K.K. thanks Professor T. Suzuki (IMS and RIKEN) for support and valuable comments in Japan.

[1] D. P. Taylor, C. F. Dion, and E. R. Bernstein, J. Chem. Phys. **106**, 3512 (1997).
[2] D. P. Taylor and E. R. Bernstein, J. Chem. Phys. **103**, 10453 (1995).
[3] D. H. Mordaunt, M. N. R. Ashford, and R. N. Dixon, J. Chem. Phys. **109**, 7659 (1998).
[4] S. A. Henck, M. A. Mason, W.-B. Yan, K. K. Lehmann, and S. L. Coy, J. Chem. Phys. **102**, 4772 (1995); **102**, 4783 (1995).
[5] J. Biesner, L. Schnieder, G. Ahlers, X. Xie, K. H. Welge, M. N. R. Ashfold, and R. N. Dixon, J. Chem. Phys. **91**, 2901 (1989).
[6] A. Nakajima, K. Fuke, K. Tsukamoto, Y. Yoshida, and K. Kaya, J. Phys. Chem. **95**, 571 (1991).
[7] T.-X. Xiang and W. A. Guillory, J. Chem. Phys. **85**, 2019 (1986).
[8] H. K. Haak and F. Stuhl, J. Phys. Chem. **88**, 3627 (1984).
[9] G. C. G. Waschewsky, D. C. Kitchen, P. W. Browning, and L. J. Butler, J. Phys. Chem. **99**, 2635 (1995).
[10] C. L. Reed, M. Kono, and M. N. R. Ashfold, J. Chem. Soc., Faraday Trans. **92**, 4897 (1996).
[11] N. Ohashi and J. T. Hougen, J. Mol. Spectrosc. **121**, 474 (1987).
[12] M. Oda, N. Ohashi, and J. T. Hougen, J. Mol. Spectrosc. **142**, 57 (1990), and references therein.
[13] T. Förster and J. C. Jurgens, Z. Phys. Chem. Abt. B **36**, 387 (1937).
[14] E. Tannenbaum, E. M. Coffin, and A. J. Harrison, J. Chem. Phys. **21**, 311 (1953).
[15] M. Tsuboi, A. Y. Hirakawa, and H. Kawashima, J. Mol. Spectrosc. **29**, 216 (1969).
[16] M. Tsuboi and A. Y. Yirakawa, Can. J. Phys. **60**, 844 (1982).
[17] G. Herzberg, *Molecular Spectra and Molecular Structure*, (Van Nostrand Reinhold, New York, 1950), Vol. 2, p. 491.
[18] R. H. Judge and D. J. Clouthier, Comput. Phys. Commun. **135**, 293 (2001).
[19] *Ab initio* calculation using the GAUSSIAN 98 program [CIS method with a 6-31++G(2*d*,2*p*) basis set] for CH_3ND_2 in the $\tilde{A}$ state gives the N–D bond length of 1.016 Å and D–N–D angle of 118.1°.